Electronic supplementary Information

Pressure-Induced Phase Behaviour and Compressibility of the Racemic and Chiral Solid Forms, Ofloxacin and Levofloxacin

Julia Gasol-Cardona,[a,b] Martin R. Ward,[b] Davide Comboni,[c] Micheal Hanfland,[c] Rebecca Scatena,[d] Mark R. Warren,[d] Andrew G.P. Maloney,[e] & Iain D.H. Oswald[a*]

[a]Strathclyde Institute of Pharmacy and Biomedical Sciences, University of Strathclyde, 161 Cathedral Street, Glasgow, G4 0RE, United Kingdom E-mail: iain.oswald@strath.ac.uk

[b]CMAC, Strathclyde Institute of Pharmacy and Biomedical Sciences, University of Strathclyde, Glasgow G1 1RD, United Kingdom

[c]European Synchrotron Radiation Facility, 71 Avenue des Martyrs, 38000 Grenoble, France

[d]Diamond Light Source, Harwell Science and Innovation Campus, Chilton, Didcot, OX11 0DE, UK

[e]The Cambridge Crystallographic Data Centre, Cambridge, CB2 1EZ, United Kingdom

Contents

S1. Solid-State Characterisation

Each of the solids was characterised prior to the pressure study to ensure the purity of the samples before the synchrotron experiments. The Pawley fits to the data indicate that the solids were a pure phase. Details of the data collection are in the main paper. The unit cell parameters were taken from the Cambridge Structural Database entries for ofloxacin (CUYCEF), levofloxacin hemihydrate (YUJNUM01) and γ-levofloxacin (LICWOM).

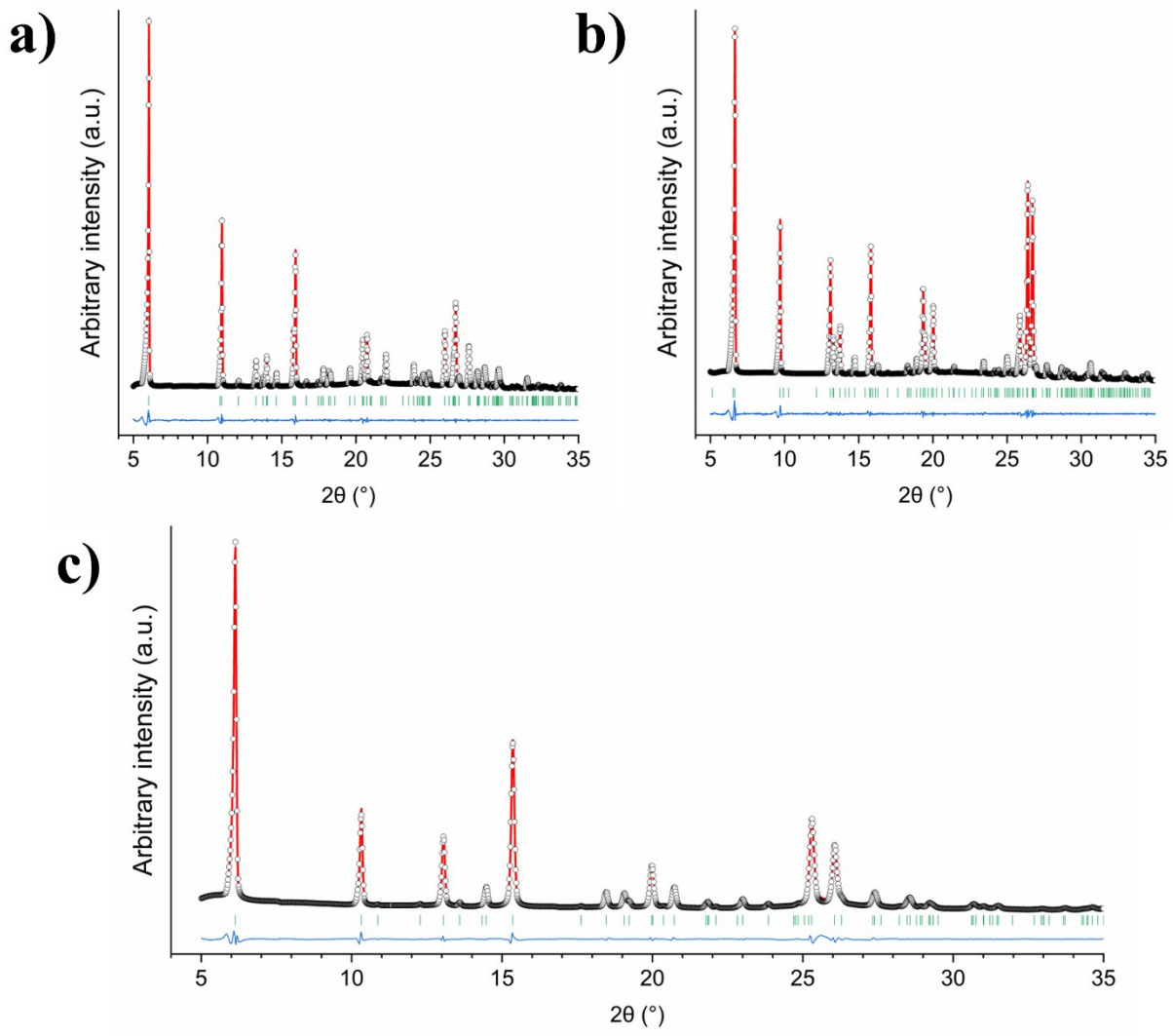

Figure S1. Pawley refinement of the powder patterns of (a) ofloxacin, (b) levofloxacin hemihydrate and (c) γ-levofloxacin collected in-house at ambient conditions.

.

Table S1. Details on the crystal structure and experimental temperature of the CSD entries for ofloxacin, γ-levofloxacin and levofloxacin hemihydrate.

	Space group	*a* (Å)	*b* (Å)	*c* (Å)	*β* (°)	Volume (Å³)	Molecular volume (Å³)	Z'	Temperature (K)
Ofloxacin CUYCEF[42]	C2/c	30.322(4)	6.8607(8)	16.9199(16)	105.271(11)	3395.6(7)	424.446	1	293
γ-Levofloxacin LICWOM[47]	C2	17.2739(10)	7.0307(2)	15.4605(8)	104.204(5)	1820.24(16)	455.060	1	423
Levofloxacin hemihydrate YUJNUM01[45]	C2	28.7580(8)	6.7988(2)	18.7648(6)	113.847(3)	3355.67(17)	419.459	2	296

Reduced Unit cell parameters

	a (Å)	*b* (Å)	*c* (Å)	*α* (°)	*β* (°)	γ (°)	Vol (Å³)
Ofloxacin CUYCEF[42]	6.861	15.544	16.920	104.89	90	102.75	1697.782
γ-Levofloxacin LICWOM[47]	7.031	9.325	15.460	103.14	90	112.15	1677.837
Levofloxacin hemihydrate YUJNUM01[45]	6.799	14.775	18.765	113.17	90	103.30	1677.837

Table S2. Experimental details

For all structures: Chemical formula: $C_{18}H_{20}FN_3O_4$, monoclinic, C2/c, Z = 8 with Mr = 361.37. Experiments were carried out at 296 K with Mo Kα radiation. Refinement was on 238 parameters with 248 restraints. H-atom parameters were constrained.

	OFLO_AMBIENT	OFLO_0p28	OFLO_0p76	OFLO_1p24
Crystal data				
a, *b*, *c* (Å)	30.251 (10), 6.8318 (8), 16.845 (2)	29.962 (13), 6.6982 (11), 16.738 (3)	29.630 (7), 6.5439 (6), 16.5404 (16)	29.425 (10), 6.4513 (8), 16.439 (2)
β (°)	105.15 (2)	104.82 (3)	104.354 (16)	104.14 (2)
V (Å^3)	3360.3 (12)	3247.3 (16)	3107.0 (9)	3026.0 (12)
μ (mm^{-1})	0.11	0.11	0.12	0.12
Crystal size (mm)	0.2 × 0.05 × 0.05	0.2 × 0.05 × 0.05	0.2 × 0.05 × 0.05	0.2 × 0.05 × 0.05
Data collection				
Absorption correction	Multi-scan	Multi-scan	Multi-scan	Multi-scan
T_{min}, T_{max}	0.625, 0.745	0.659, 0.745	0.671, 0.745	0.672, 0.745
No. of measured, independent and observed [$I > 2\sigma(I)$] reflections	5571, 826, 450	3332, 803, 430	5492, 792, 493	5594, 773, 486
R_{int}	0.079	0.064	0.073	0.071
θ_{max} (°)	23.3	23.2	23.3	23.3
$(\sin\theta/l)_{max}$ (Å^{-1})	0.557	0.554	0.556	0.556
Refinement				
$R[F^2 > 2\sigma(F^2)]$, $wR(F^2)$, S	0.042, 0.106, 1.03	0.043, 0.105, 1.03	0.042, 0.115, 1.15	0.049, 0.134, 1.11
No. of reflections	826	803	792	773
	$w = 1/[\sigma^2(F_o^2) + (0.0428P)^2 + 2.724P]$ where $P = (F_o^2 + 2F_c^2)/3$	$w = 1/[\sigma^2(F_o^2) + (0.049P)^2]$ where $P = (F_o^2 + 2F_c^2)/3$	$w = 1/[\sigma^2(F_o^2) + (0.0594P)^2 + 0.4936P]$ where $P = (F_o^2 + 2F_c^2)/3$	$w = 1/[\sigma^2(F_o^2) + (0.0386P)^2 + 15.8378P]$ where $P = (F_o^2 + 2F_c^2)/3$
ρ_{max}, ρ_{min} (e Å^{-3})	0.08, -0.09	0.10, -0.09	0.10, -0.10	0.14, -0.17

	OFLO_1p81	OFLO-2p16	OFLO_2p47	OFLO_3p0

Crystal data				
a, b, c (Å)	29.123 (7), 6.3326 (6), 16.2627 (16)	29.051 (7), 6.2990 (6), 16.2226 (17)	28.984 (8), 6.2603 (6), 16.1666 (16)	28.803 (7), 6.1832 (5), 16.0548 (14)
β (°)	103.781 (17)	103.694 (16)	103.600 (18)	103.372 (15)
V (Å^3)	2912.9 (9)	2884.3 (9)	2851.2 (9)	2781.8 (7)
μ (mm^{-1})	0.13	0.13	0.13	0.13
Crystal size (mm)	0.2 × 0.05 × 0.05	0.2 × 0.05 × 0.05	0.2 × 0.05 × 0.05	0.2 × 0.05 × 0.05
Data collection				
Absorption correction	Multi-scan	Multi-scan	Multi-scan	Multi-scan
T_{min}, T_{max}	0.665, 0.745	0.677, 0.745	0.670, 0.745	0.681, 0.745
No. of measured, independent and observed [$I > 2\sigma(I)$] reflections	5261, 737, 490	4013, 719, 486	5267, 714, 495	5369, 692, 497
R_{int}	0.064	0.060	0.067	0.061
θ_{max} (°)	23.3	23.3	23.3	23.3
$(\sin\theta/l)_{max}$ (Å^{-1})	0.557	0.557	0.556	0.556
Refinement				
$R[F^2 > 2\sigma(F^2)]$, $wR(F^2)$, S	0.045, 0.127, 1.12	0.042, 0.117, 1.11	0.039, 0.079, 1.15	0.036, 0.082, 1.10
No. of reflections	737	719	714	692
	$w = 1/[\sigma^2(F_o^2) + (0.0763P)^2 + 1.4703P]$ where $P = (F_o^2 + 2F_c^2)/3$	$w = 1/[\sigma^2(F_o^2) + (0.0649P)^2 + 1.7593P]$ where $P = (F_o^2 + 2F_c^2)/3$	$w = 1/[\sigma^2(F_o^2) + (0.0201P)^2 + 5.3119P]$ where $P = (F_o^2 + 2F_c^2)/3$	$w = 1/[\sigma^2(F_o^2) + (0.0216P)^2 + 7.593P]$ where $P = (F_o^2 + 2F_c^2)/3$
ρ_{max}, ρ_{min} (e Å^{-3})	0.19, -0.14	0.12, -0.11	0.15, -0.13	0.12, -0.12

	OFLO_3p62	OFLO_4p47	OFLO_5p2
Crystal data			

a, *b*, *c* (Å)	28.697 (7), 6.1346 (5), 15.9813 (14)	28.547 (7), 6.0686 (5), 15.8759 (14)	28.443 (9), 6.0167 (7), 15.7781 (17)
β (°)	103.278 (15)	103.121 (16)	102.951 (18)
V (Å^3)	2738.2 (7)	2678.6 (8)	2631.5 (10)
μ (mm^{-1})	0.13	0.14	0.14
Crystal size (mm)	0.2 × 0.05 × 0.05	0.2 × 0.05 × 0.05	0.2 × 0.05 × 0.05
Data collection			
Absorption correction	Multi-scan	Multi-scan	Multi-scan
T_{min}, T_{max}	0.646, 0.745	0.679, 0.745	0.669, 0.745
No. of measured, independent and observed [$I > 2\sigma(I)$] reflections	4764, 686, 483	4915, 672, 478	3791, 666, 469
R_{int}	0.060	0.061	0.057
θ_{max} (°)	23.3	23.3	23.3
$(\sin \theta/l)_{max}$ (Å^{-1})	0.556	0.556	0.556
Refinement			
$R[F^2 > 2\sigma(F^2)]$, $wR(F^2)$, S	0.038, 0.097, 1.11	0.038, 0.093, 1.10	0.031, 0.084, 1.05
No. of reflections	686	672	666
	$w = 1/[\sigma^2(F_o^2) + (0.0446P)^2 + 4.3269P]$ where $P = (F_o^2 + 2F_c^2)/3$	$w = 1/[\sigma^2(F_o^2) + (0.0282P)^2 + 9.9383P]$ where $P = (F_o^2 + 2F_c^2)/3$	$w = 1/[\sigma^2(F_o^2) + (0.0534P)^2 + 0.3586P]$ where $P = (F_o^2 + 2F_c^2)/3$
ρ_{max}, ρ_{min} (e Å^{-3})	0.15, -0.14	0.13, -0.14	0.10, -0.13

Table S3. Experimental details

For all structures: Chemical formula: $C_{18}H_{20}FN_3O_4 \cdot 0.5(H_2O)$, monoclinic, C2, Z = 8 with Mr = 370.38. Experiments were carried out at 298 K with Mo Kα radiation. Refinement was on 225 parameters with 123 restraints. H-atom parameters were constrained.

	LH_ME_0p38	LH_ME_0p84	LH_ME_1p17	LH_ME_1p68
Crystal data				
a, *b*, *c* (Å)	28.512 (5), 6.7261 (4), 18.5315 (13)	28.224 (4), 6.6179 (4), 18.353 (1)	28.099 (5), 6.5600 (4), 18.2689 (11)	27.928 (5), 6.4713 (4), 18.1487 (13)

β (°)	113.557 (12)	113.462 (9)	113.434 (10)	113.447 (12)
V (Å^3)	3257.7 (7)	3144.6 (6)	3089.7 (6)	3009.2 (7)
μ (mm^{-1})	0.12	0.12	0.12	0.13
Crystal size (mm)	0.18 × 0.09 × 0.02	0.18 × 0.09 × 0.02	0.18 × 0.09 × 0.02	0.18 × 0.09 × 0.02
Data collection				
Absorption correction	Multi-scan	Multi-scan	Multi-scan	Multi-scan
T_{min}, T_{max}	0.668, 0.745	0.668, 0.745	0.668, 0.745	0.668, 0.745
No. of measured, independent and observed [I > 2σ(I)] reflections	7699, 1529, 1116	7420, 1472, 1134	7304, 1447, 1151	7133, 1399, 1128
R_{int}	0.046	0.044	0.044	0.045
θ_{max} (°)	23.3	23.4	23.4	23.3
(sin θ/l)$_{max}$ (Å^{-1})	0.557	0.558	0.558	0.556
Refinement				
R[F^2 > 2σ(F^2)], wR(F^2), S	0.080, 0.259, 1.07	0.070, 0.209, 1.08	0.065, 0.197, 1.07	0.060, 0.178, 1.04
No. of reflections	1529	1472	1447	1399
ρ_{max}, ρ_{min} (e Å^{-3})	0.28, -0.33	0.21, -0.25	0.21, -0.22	0.20, -0.22
Absolute structure	Flack x determined using 393 quotients [(I+)-(I-)]/[(I+)+(I-)] (Parsons, Flack and Wagner, Acta Cryst. B69 (2013) 249-259).	Flack x determined using 403 quotients [(I+)-(I-)]/[(I+)+(I-)] (Parsons, Flack and Wagner, Acta Cryst. B69 (2013) 249-259).	Flack x determined using 423 quotients [(I+)-(I-)]/[(I+)+(I-)] (Parsons, Flack and Wagner, Acta Cryst. B69 (2013) 249-259).	Flack x determined using 406 quotients [(I+)-(I-)]/[(I+)+(I-)] (Parsons, Flack and Wagner, Acta Cryst. B69 (2013) 249-259).
Absolute structure parameter	0.7 (10)	-0.1 (10)	-1.0 (10)	-1.1 (10)

	LH_ME_2p27
Crystal data	

a, *b*, *c* (Å)	27.806 (6), 6.4028 (5), 18.0642 (15)
β (°)	113.520 (14)
V (Å^3)	2948.9 (8)
μ (mm^{-1})	0.13
Crystal size (mm)	0.18 × 0.09 × 0.02
Data collection	
Absorption correction	Multi-scan
T_{min}, T_{max}	0.668, 0.745
No. of measured, independent and observed [$I > 2\sigma(I)$] reflections	6966, 1377, 1115
R_{int}	0.044
θ_{max} (°)	23.3
$(\sin \theta/\lambda)_{max}$ (Å^{-1})	0.557
Refinement	
$R[F^2 > 2\sigma(F^2)]$, $wR(F^2)$, S	0.056, 0.149, 1.05
No. of reflections	1377
ρ_{max}, ρ_{min} (e Å^{-3})	0.19, -0.22
Absolute structure	Flack x determined using 405 quotients [(I+)-(I-)]/[(I+)+(I-)] (Parsons, Flack and Wagner, Acta Cryst. B69 (2013) 249-259).
Absolute structure parameter	-0.4 (10)

Table S4. Experimental details

For most structures: Chemical formula: $C_{18}H_{20}FN_3O_4 \cdot 0.5(H_2O)$, monoclinic, C2, Z = 8 with Mr = 370.38. The highest pressure structure is observed in triclinic P1. Experiments were carried out at 298 K with Mo Kα radiation. Refinement was on 225 parameters with 123 restraints for low-pressure phase and 396 parameters with 114 restraints for the high-pressure phase. H-atom parameters were constrained.

	LH_PE_0p29	LH_PE_1p26	LH_PE_2p19	LH_PE_2p4
Crystal data				
a, *b*, *c* (Å)	28.753 (4),	28.1035 (17),	27.878 (3),	27.834 (2),

	6.7900 (8), 18.636 (5)	6.5548 (4), 18.263 (2)	6.4360 (6), 18.107 (3)	6.4010 (5), 18.072 (3)
β (°)	113.838 (11)	113.490 (4)	113.447 (8)	113.524 (5)
V (Å^3)	3328.0 (10)	3085.5 (5)	2980.5 (7)	2952.2 (5)
Z	8	8	8	8
μ (mm^{-1})	0.12	0.12	0.13	0.13
Crystal size (mm)	0.18 × 0.09 × 0.02	0.18 × 0.09 × 0.02	0.18 × 0.09 × 0.02	0.18 × 0.09 × 0.02
Data collection				
Absorption correction	Multi-scan SADABS2016/2 (Bruker,2016/2) was used for absorption correction. wR2(int) was 0.0723 before and 0.0600 after correction. The Ratio of minimum to maximum transmission is 0.8619. The λ/2 correction factor is Not present.	Multi-scan SADABS2016/2 (Bruker,2016/2) was used for absorption correction. wR2(int) was 0.0688 before and 0.0592 after correction. The Ratio of minimum to maximum transmission is 0.8644. The λ/2 correction factor is Not present.	Multi-scan SADABS2016/2 (Bruker,2016/2) was used for absorption correction. wR2(int) was 0.0943 before and 0.0627 after correction. The Ratio of minimum to maximum transmission is 0.8671. The λ/2 correction factor is Not present.	Multi-scan SADABS2016/2 (Bruker,2016/2) was used for absorption correction. wR2(int) was 0.0683 before and 0.0586 after correction. The Ratio of minimum to maximum transmission is 0.8423. The λ/2 correction factor is Not present.
Tmin, Tmax	0.642, 0.745	0.644, 0.745	0.646, 0.745	0.628, 0.745
No. of measured, independent and observed [$I > 2\sigma(I)$] reflections	14088, 3365, 1849	14280, 3200, 2189	7275, 2495, 1706	15574, 3158, 2411
R_{int}	0.083	0.065	0.058	0.057
θ_{max} (°)	24.8	24.8	23.3	24.7
$(\sin\theta/l)_{max}$ (Å^{-1})	0.590	0.589	0.555	0.588
Refinement				
$R[F^2 > 2\sigma(F^2)]$, $wR(F^2)$, S	0.096, 0.323, 1.07	0.079, 0.264, 1.03	0.065, 0.184, 1.03	0.069, 0.197, 1.06
No. of reflections	3365	3200	2495	3158

ρ_{max}, ρ_{min} (e Å^{-3})	0.52, -0.35	0.54, -0.55	0.27, -0.31	0.40, -0.46
Absolute structure	Flack x determined using 609 quotients [(I+)-(I-)]/[(I+)+(I-)] (Parsons, Flack and Wagner, Acta Cryst. B69 (2013) 249-259).	Flack x determined using 757 quotients [(I+)-(I-)]/[(I+)+(I-)] (Parsons, Flack and Wagner, Acta Cryst. B69 (2013) 249-259).	Flack x determined using 560 quotients [(I+)-(I-)]/[(I+)+(I-)] (Parsons, Flack and Wagner, Acta Cryst. B69 (2013) 249-259).	Flack x determined using 877 quotients [(I+)-(I-)]/[(I+)+(I-)] (Parsons, Flack and Wagner, Acta Cryst. B69 (2013) 249-259).
Absolute structure parameter	0.5 (10)	-0.7 (8)	-0.3 (10)	0.1 (6)

	LH_PE_2p99	LH_PE_4p05	LH_PE_5p98
Crystal data			
a, *b*, *c* (Å)	27.717 (3), 6.3111 (6), 17.983 (4)	27.562 (3), 6.1945 (7), 17.830 (4)	13.985 (2), 6.0616 (6), 17.534 (3)
α, β, γ (°)	113.633 (9)	113.823 (9)	81.661 (9), 109.861 (12), 79.082 (7)
V (Å^3)	2881.9 (7)	2784.7 (8)	1336.9 (3)
Z	8	8	4
μ (mm^{-1})	0.13	0.14	0.14
Crystal size (mm)	0.18 × 0.09 × 0.02	0.18 × 0.09 × 0.02	0.18 × 0.09 × 0.02
Data collection			
Absorption correction	Multi-scan SADABS2016/2 (Bruker,2016/2) was used for absorption correction. wR2(int) was 0.0838 before and 0.0593 after correction. The Ratio of minimum to maximum transmission is 0.847. The λ/2 correction factor is Not present.	Multi-scan SADABS2016/2 (Bruker,2016/2) was used for absorption correction. wR2(int) was 0.1083 before and 0.0908 after correction. The Ratio of minimum to maximum transmission is 0.837. The λ/2 correction factor is Not present.	Multi-scan SADABS2016/2 (Bruker,2016/2) was used for absorption correction. wR2(int) was 0.0683 before and 0.0586 after correction. The Ratio of minimum to maximum transmission is 0.8803. The λ/2 correction factor is Not present.
Tmin, Tmax	0.631, 0.745	0.617, 0.737	0.656, 0.745

No. of measured, independent and observed [$I > 2\sigma(I)$] reflections	11056, 3011, 1993	13522, 2926, 1973	7462, 2614, 1587
R_{int}	0.081	0.089	0.057
θ_{max} (°)	24.8	24.9	23.3
$(\sin \theta/l)_{max}$ (Å^{-1})	0.590	0.591	0.556
Refinement			
$R[F^2 > 2\sigma(F^2)]$, $wR(F^2)$, S	0.073, 0.234, 1.13	0.107, 0.327, 1.20	0.086, 0.276, 1.01
No. of reflections	3011	2926	2614
ρ_{max}, ρ_{min} (e Å^{-3})	0.53, -0.41	0.49, -0.62	0.32, -0.36
Absolute structure	Flack x determined using 647 quotients [(I+)-(I-)]/[(I+)+(I-)] (Parsons, Flack and Wagner, Acta Cryst. B69 (2013) 249-259).	Flack x determined using 637 quotients [(I+)-(I-)]/[(I+)+(I-)] (Parsons, Flack and Wagner, Acta Cryst. B69 (2013) 249-259).	Flack x determined using 608 quotients [(I+)-(I-)]/[(I+)+(I-)] (Parsons, Flack and Wagner, Acta Cryst. B69 (2013) 249-259).
Absolute structure parameter	-0.4 (10)	-1.8 (10)	0.6 (10)

Table S5. Refined unit cell parameters for ofloxacin in a methanol–ethanol mixture.

XRPD file number, ESRF	Pressure (GPa)	a-axis (Å)	a-axis error (Å)	b-axis (Å)	b-axis error (Å)	c-axis (Å)	c-axis error (Å)	β-angle (°)	β-angle error (°)	Unt cell volume (Å^3)	Unit cell volume error (Å^3)
Inhouse PXRD	0.00	30.3166	0.0013	6.8479	0.0001	16.8687	0.0006	105.146	0.003	3380.4	0.2
2	0.11	30.1251	0.0012	6.7686	0.0002	16.7826	0.0007	104.953	0.002	3306.2	0.2
8	0.32	29.9005	0.0012	6.6754	0.0002	16.6813	0.0007	104.733	0.002	3220.1	0.2
13	0.41	29.8275	0.0013	6.6482	0.0002	16.6468	0.0006	104.670	0.002	3193.4	0.2
20	0.46	29.7858	0.0015	6.6379	0.0002	16.6369	0.0007	104.649	0.003	3182.5	0.2
22	0.68	29.6298	0.0014	6.5644	0.0002	16.5510	0.0007	104.456	0.003	3117.3	0.2
26	0.80	29.5676	0.0013	6.5393	0.0002	16.5221	0.0007	104.394	0.003	3094.3	0.2
34	0.95	29.4862	0.0013	6.5100	0.0002	16.4868	0.0008	104.312	0.003	3066.5	0.2
38	1.13	29.3962	0.0015	6.4724	0.0003	16.4395	0.0009	104.214	0.004	3032.1	0.3
43	1.32	29.3325	0.0017	6.4466	0.0004	16.4075	0.0011	104.152	0.004	3008.4	0.3
47	1.57	29.2449	0.0014	6.4087	0.0003	16.3598	0.0008	104.053	0.003	2974.4	0.3
51	1.68	29.2014	0.0018	6.3934	0.0004	16.3375	0.0010	104.000	0.003	2959.5	0.3
55	1.86	29.1421	0.0016	6.3710	0.0003	16.3072	0.0010	103.951	0.003	2938.4	0.3
58	1.99	29.093	0.002	6.3548	0.0004	16.2800	0.0012	103.901	0.004	2921.7	0.4
68	2.10	29.051	0.002	6.3482	0.0004	16.2720	0.0012	103.889	0.004	2913.1	0.3
70	2.28	28.997	0.003	6.3197	0.0006	16.2331	0.0016	103.794	0.005	2888.9	0.5
73	2.52	28.913	0.002	6.2907	0.0004	16.1945	0.0013	103.711	0.004	2861.5	0.4
88	2.70	28.845	0.003	6.2848	0.0003	16.1802	0.0012	103.695	0.005	2849.8	0.4
95	2.99	28.752	0.003	6.2447	0.0005	16.1192	0.0015	103.582	0.006	2813.3	0.5
97	3.44	28.660	0.003	6.1922	0.0004	16.0499	0.0014	103.425	0.006	2770.5	0.4
100	3.81	28.575	0.002	6.1641	0.0003	16.0047	0.0011	103.365	0.006	2742.7	0.3
104	4.12	28.524	0.003	6.1324	0.0003	15.9601	0.0012	103.262	0.006	2717.3	0.3
106	4.65	28.457	0.003	6.0955	0.0003	15.9015	0.0012	103.157	0.006	2685.9	0.4

Table S6. Refined unit cell parameters for ofloxacin in petroleum ether.

XRPD file number, ESRF	Pressure (GPa)	a-axis (Å)	a-axis error (Å)	b-axis (Å)	b-axis error (Å)	c-axis (Å)	c-axis error (Å)	β-angle (°)	β-angle error (°)	Unit cell volume (Å^3)	Unit cell volume error (Å^3)
Inhouse PXRD	0.00	30.3166	0.0013	6.8479	0.0001	16.8687	0.0006	105.146	0.003	3380.4	0.2
7	0.21	29.9815	0.0016	6.7157	0.0003	16.7244	0.0009	104.830	0.003	3255.3	0.3
9	0.34	29.8650	0.0017	6.6654	0.0002	16.6721	0.0008	104.707	0.003	3210.0	0.3
11	0.50	29.7365	0.0019	6.6108	0.0003	16.6075	0.0010	104.565	0.004	3159.8	0.3
14	0.71	29.6066	0.0018	6.5539	0.0002	16.5425	0.0009	104.422	0.004	3108.8	0.3
21	0.99	29.445	0.002	6.4923	0.0003	16.4642	0.0011	104.276	0.005	3050.2	0.3
23	1.38	29.2854	0.0016	6.4173	0.0003	16.3728	0.0009	104.062	0.003	2984.8	0.3
25	1.64	29.1849	0.0016	6.3742	0.0003	16.3158	0.0009	103.949	0.003	2945.7	0.3
27	2.08	29.0473	0.0014	6.3151	0.0002	16.2371	0.0007	103.779	0.003	2892.8	0.2
32	2.34	28.9828	0.0014	6.2883	0.0002	16.1990	0.0008	103.708	0.003	2868.2	0.2
35	2.73	28.8782	0.0016	6.2412	0.0004	16.1302	0.0011	103.583	0.003	2825.9	0.3
42	2.97	28.8043	0.0015	6.2272	0.0002	16.1027	0.0008	103.535	0.003	2808.1	0.2
45	3.25	28.7523	0.0016	6.2030	0.0003	16.0680	0.0008	103.454	0.004	2787.1	0.2
50	3.55	28.6716	0.0018	6.1834	0.0003	16.0331	0.0009	103.405	0.004	2765.0	0.3
52	3.81	28.6190	0.0019	6.1602	0.0003	15.9985	0.0009	103.348	0.004	2744.3	0.3
58	4.05	28.550	0.002	6.1413	0.0003	15.9646	0.0009	103.290	0.004	2724.2	0.3
66	4.39	28.489	0.002	6.1200	0.0003	15.9306	0.0010	103.218	0.005	2704.0	0.3
73	4.69	28.421	0.003	6.0985	0.0003	15.8946	0.0011	103.145	0.006	2682.8	0.4
76	5.59	28.305	0.007	6.0528	0.0006	15.8136	0.0019	102.997	0.010	2639.9	0.8
79	5.96	28.249	0.008	6.0345	0.0006	15.773	0.002	102.963	0.011	2620.4	0.9
80	6.23	28.230	0.010	6.0283	0.0007	15.759	0.002	102.918	0.012	2614.0	1.0

Table S7. Refined unit cell parameters for levofloxacin hemihydrate in a methanol–ethanol mixture.

XRPD file number, ESRF	Pressure (GPa)	a-axis (Å)	a-axis error (Å)	b-axis (Å)	b-axis error (Å)	c-axis (Å)	c-axis error (Å)	β-angle (°)	β-angle error (°)	Unit cell volume (Å^3)	Unit cell volume error (Å^3)
Inhouse PXRD	0	29.1183	0.0015	6.8832	0.0002	18.8462	0.0008	114.066	0.003	3449.0	0.3
5	0	29.190	0.003	6.8948	0.0004	18.8798	0.0019	114.166	0.007	3466.7	0.6
8	0.15	28.937	0.004	6.8357	0.0006	18.759	0.004	113.905	0.012	3392.4	0.9
11	0.45	28.691	0.006	6.7621	0.0011	18.611	0.004	113.725	0.011	3305.5	1.1
14	0.70	28.487	0.003	6.7034	0.0005	18.5060	0.0019	113.587	0.007	3238.7	0.6
17	0.72	28.456	0.003	6.6956	0.0005	18.4970	0.0018	113.591	0.007	3229.7	0.6
23	1.08	28.255	0.003	6.6127	0.0003	18.376	0.002	113.550	0.008	3147.4	0.6
29	1.39	28.114	0.003	6.5531	0.0007	18.2746	0.0017	113.490	0.008	3087.7	0.6
35	1.80	28.033	0.004	6.4860	0.0007	18.203	0.003	113.562	0.009	3033.8	0.7
41	2.22	27.888	0.003	6.4165	0.0004	18.1004	0.0015	113.528	0.007	2969.6	0.5
47	2.87	27.772	0.003	6.3388	0.0005	18.0044	0.0017	113.585	0.008	2904.7	0.5
56	3.21	27.707	0.004	6.3144	0.0006	17.964	0.003	113.553	0.011	2881.1	0.7
59	3.86	27.620	0.005	6.2553	0.0008	17.891	0.003	113.587	0.012	2832.8	0.8

Table S8. Refined unit cell parameters for levofloxacin hemihydrate in petroleum ether.

XRPD file number, ESRF	Pressure (GPa)	a-axis (Å)	a-axis error (Å)	b-axis (Å)	b-axis error (Å)	c-axis (Å)	c-axis error (Å)	β-angle (°)	β-angle error (°)	Unit cell volume (Å^3)	Unit cell volume error (Å^3)
In-house PXRD	0.00	29.1183	0.0015	6.8832	0.0002	18.8462	0.0008	114.066	0.003	3449.0	0.3
5	0.00	29.190	0.003	6.8948	0.0004	18.8798	0.0019	114.166	0.007	3466.7	0.6
2	0.32	28.676	0.005	6.7703	0.0012	18.622	0.004	113.709	0.010	3310.2	1.1
12	0.60	28.404	0.003	6.6871	0.0005	18.455	0.002	113.524	0.006	3214.1	0.5
14	0.73	28.340	0.003	6.6636	0.0005	18.417	0.002	113.503	0.006	3189.5	0.6
23	1.28	28.089	0.004	6.5485	0.0009	18.253	0.002	113.458	0.006	3079.9	0.7
25	1.74	27.948	0.004	6.4745	0.0007	18.150	0.002	113.450	0.007	3012.9	0.7
36	2.26	27.850	0.005	6.4170	0.0011	18.082	0.004	113.475	0.009	2964.1	0.9
41	2.46	27.809	0.004	6.3882	0.0008	18.038	0.003	113.474	0.009	2939.3	0.8
45	3.18	27.676	0.004	6.3078	0.0006	17.939	0.003	113.533	0.009	2871.3	0.7

Table S9. Refined unit cell parameters for γ-levofloxacin in a methanol–ethanol mixture.

XRPD file number, ESRF	Pressure (GPa)	a-axis (Å)	a-axis error (Å)	b-axis (Å)	b-axis error (Å)	c-axis (Å)	c-axis error (Å)	β-angle (°)	β-angle error (°)	Unit cell volume (Å^3)	Unit cell volume error (Å^3)
Inhouse PXRD	0.00	17.503	0.003	7.0367	0.0013	14.720	0.003	101.845	0.008	1774.3	0.6
11	0.31	17.4770	0.0016	6.9550	0.0003	14.850	0.002	102.508	0.008	1762.2	0.3
17	0.41	17.467	0.004	6.9204	0.0011	14.839	0.006	102.74	0.02	1749.5	0.8
24	0.52	17.464	0.003	6.8757	0.0007	14.821	0.004	103.020	0.013	1733.9	0.6
25	0.64	17.451	0.004	6.8336	0.0010	14.782	0.005	103.251	0.015	1715.9	0.7
28	0.75	17.448	0.006	6.8032	0.0017	14.754	0.005	103.421	0.018	1703.6	0.9
33	0.88	17.444	0.006	6.7736	0.0018	14.700	0.005	103.52	0.02	1688.8	0.9
39	1.14	17.520	0.009	6.7312	0.0024	14.708	0.006	103.97	0.02	1686.7	1.2
45	1.32	17.519	0.005	6.7078	0.0011	14.696	0.005	104.00	0.02	1675.6	0.8

48	1.63	17.497	0.004	6.6712	0.0009	14.626	0.005	104.10	0.02	1655.8	0.7
58	1.92	17.518	0.006	6.6431	0.0013	14.571	0.00	104.29	0.02	1643.2	1.1
61	2.30	17.463	0.010	6.597	0.003	14.455	0.008	104.42	0.03	1612.9	1.4
67	2.70	17.479	0.007	6.5697	0.0019	14.416	0.008	104.59	0.02	1602.0	1.2
68	3.17	17.447	0.013	6.537	0.004	14.364	0.009	104.70	0.03	1584.6	1.8
73	3.86	17.45	0.06	6.50	0.02	14.34	0.05	104.91	0.03	1571	9
77	4.33	17.41	0.02	6.467	0.006	14.259	0.015	104.93	0.03	1551	3
88	4.97	17.39	0.03	6.433	0.008	14.20	0.02	105.00	0.03	1534	4
90	5.73	17.38	0.03	6.411	0.009	14.15	0.02	105.07	0.03	1522	4

The data for γ-levofloxacin in petroleum ether was largely the levofloxacin hemihydrate so no parameters determined.

Table S10. Table displaying the total lattice energies (E_{tot}) of ofloxacin (CUYCEF) and γ-levofloxacin (LICWOM) at ambient pressure, along with the partitioning into Coulombic energy (E_{Coul}), polarisation energy (E_{pol}), dispersion energy (E_{disp}) and repulsion energy (E_{rep}). All energies are represented in kJ mol^{-1}.

CSD ref code	E_{Coul}	E_{pol}	E_{disp}	E_{rep}	E_{tot}
CUYCEF	-70.9	-28.6	-157.4	101	-156
LICWOM	-65.7	-30.9	-134.2	119	-112

S2. Sapphire Capillary Cell

The sapphire capillary cell enabled us to explore the pressure regime from 1 bar to 1200 bar. We modified the standard process by using narrow pieces of Kapton film rather than the previous method of carbon fibres. The advantage of this technique was that the crystals could be visualised better to enable quicker centring. We created small cuts in the film so that these could also be used to aid alignment. We took the opportunity to load two to three crystals so that for every pressure point we could collect data on multiple crystals by moving the z-stage of the goniometer, reducing the time spent loading cells.

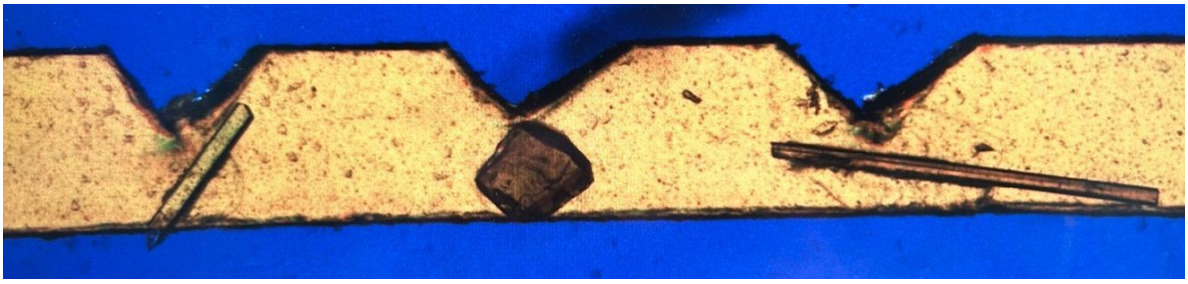

Figure S2. Kapton film modification developed during beamtime to reduce the downtime for loading.

S3. Compression of O, LH and Lγ

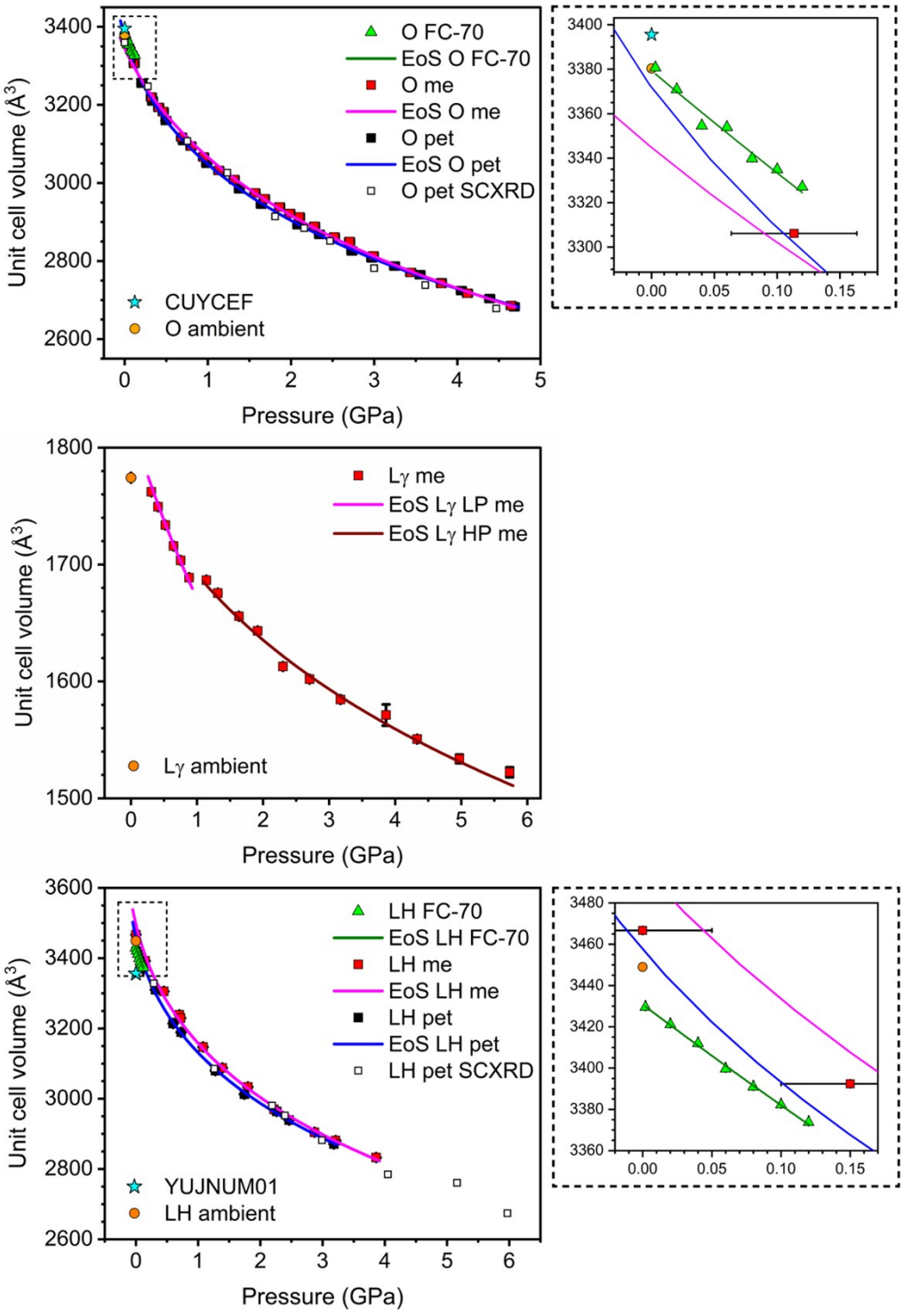

Figure S3. Change in the unit cell volume of ofloxacin (O), γ-levofloxacin (Lγ) and levofloxacin hemihydrate (LH) as a function of pressure. Data points include errors in unit cell volume and pressure. Volumes were fitted using the equations of state listed in Table S11. For Lγ, volumes before and after the suspected phase transition were fitted separately as low-pressure (LP) and high-pressure (HP) phases. Unit cell volumes of CSD entries for ofloxacin (CUYCEF) and levofloxacin hemihydrate (YUJNUM01) are included. Unit cell volumes of ambient in-house XRPD data are included. Samples were compressed in Fluorinert ™ FC-70 (FC-70), a methanol–ethanol mixture (me) and petroleum ether (pet). Overlaid are the unit cell volumes for the single crystal measurements (black unfilled squares). For LH, the unit cell volume of the high-pressure phase is multiplied by 2 to equate to the low-pressure form.

Table S11. Fitting parameters of the equations of state for ofloxacin (O), γ-levofloxacin (Lγ) and levofloxacin hemihydrate (LH) from pressure studies carried out in a methanol–ethanol mixture (me), petroleum ether (pet) and Fluorinert ™ FC-70 (FC-70). Powder and single crystal samples were studied using diamond anvil cells and a sapphire capillary cell (SCC). Lγ was fitted using the data to 0.88 GPa (before the suspected phase transition). The volumes have been set to be the measured pressures at ambient pressure and fixed based on suggestions of the referee. 2nd-order fits to the powder diffraction studies did not describe the data as well as the 3rd -order with volumes fixed.

	Fitted EoS	V_0	K_0	K'
O me (XRPD) 0-4.65 GPa	3rd Vinet	3337(11)	8.0(6)	9.3(4)
O pet (XRPD) 0-6.23 GPa	3rd Vinet	3358(16)	5.9(5)	11.8(4)
O me (SCXRD) 0-5.20 GPa	3rd Vinet	3368(24)	6.4(8)	10.0(6)
O SCC FC-70 (SCXRD) 0.003-0.12 GPa	2nd Vinet	3379(3)	7.3(6)	1*
LH me (XRPD) 0-3.86 GPa	3rd Vinet	3490(22)	5.6(8)	11.6(9)
LH pet (XRPD) 0-3.18 GPa	3rd Vinet	3456(26)	5.4(10)	12.9(12)
LH me (SCXRD) 0-2.23 GPa	3rd Vinet	3451	3.6(7)	26(7)
LH SCC FC-70 (SCXRD) 0.002-0.12 GPa	2nd Vinet	3430.6(8)	6.96(17)	1*
Lγ me (XRPD) 0-0.88 GPa$	2nd Vinet	1805(9)	12.6(14)	1*
Lγ me (XRPD) 1.1-5.8 GPa* **	3rd Vinet	1767.5(18)	18.1(11)	9.3(12)

*K' is set to 1 in 2nd order Vinet Equation of State hence no error is associated with this value.

$The data point at 0.0001 GPa was not used in the fit.

***2nd-order fit does not represent the data well. The refinement of all three parameters was unstable. K_0 and K' were refined based on estimated volume of 1766.5. The V_0 was refined with values of K0 and K' fixed. This was iteratively done. Whilst the errors in the values are likely underestimated, it provides a reasonable fit to the experimental data.

Table S12. Principal axes of strain for the crystal structures of ofloxacin (O), γ-levofloxacin (Lγ) and levofloxacin hemihydrate (LH) based on the compression of powder samples in a methanol–ethanol mixture. The table displays the direction of compression and the coefficient of compressibility (K).

	PRINCIPAL AXES OF STRAIN					
	X1		X2		X3	
	Direction	**K** (TPa^{-1})	**Direction**	**K** (TPa^{-1})	**Direction**	**K** (TPa^{-1})
O	[0,1,0]	23.2(2)	[-0.6082, 0, 0.7938]	15.1(1)	[0.4196, 0, 0.9077]	7.89(7)
Lγ	[0,1,0]	17.3(3)	[0.4782, 0, 0.8783]	14.1(6)	[0.8651, 0, -0.5015]	-0.1(6)
LH	[0,1,0]	31.4(5)	[0.8115, 0, -0.5844]	16.8(5)	[0.4294, 0, 0.9031]	14.9(2)

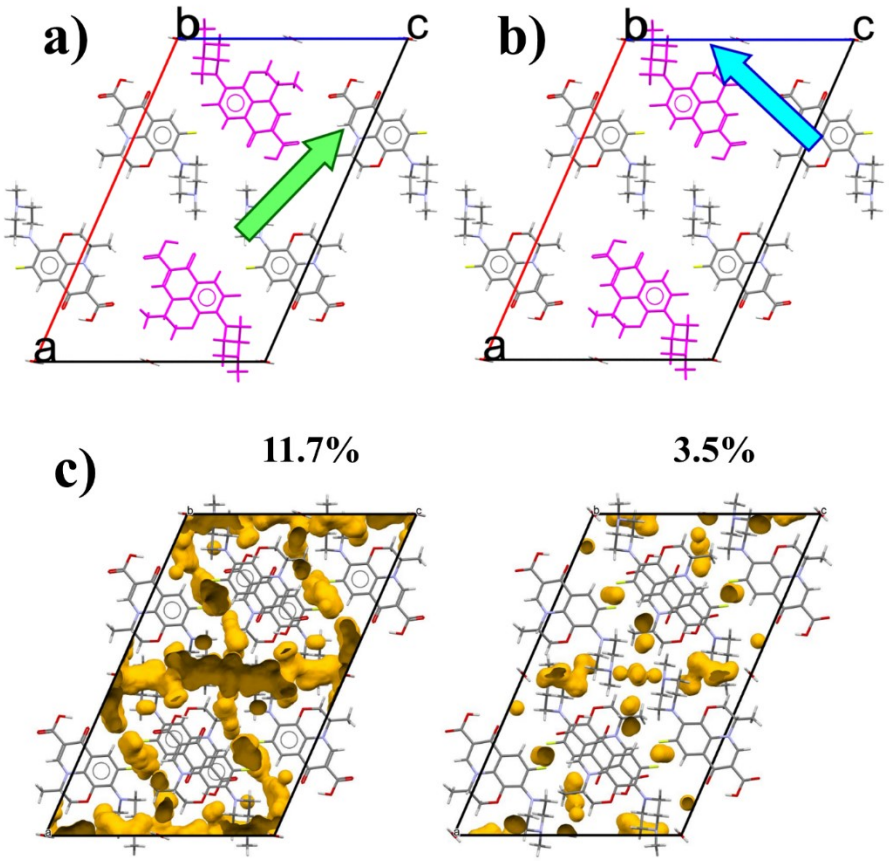

Figure S4. (Top) Depictions of the directions of (a) median (green arrow) and (b) minimum (blue arrow) principal compressibilities in levofloxacin hemihydrate. The neutral and pink molecular colouring indicates the different conformers in the unit cell. (Bottom) c) Depiction of voids in levofloxacin hemihydrate at ambient pressure (left; YUJNUM01) and 2.27 GPa (right) (Mercury void analysis using 0.6 Å probe radius and a grid spacing of 0.2 Å).

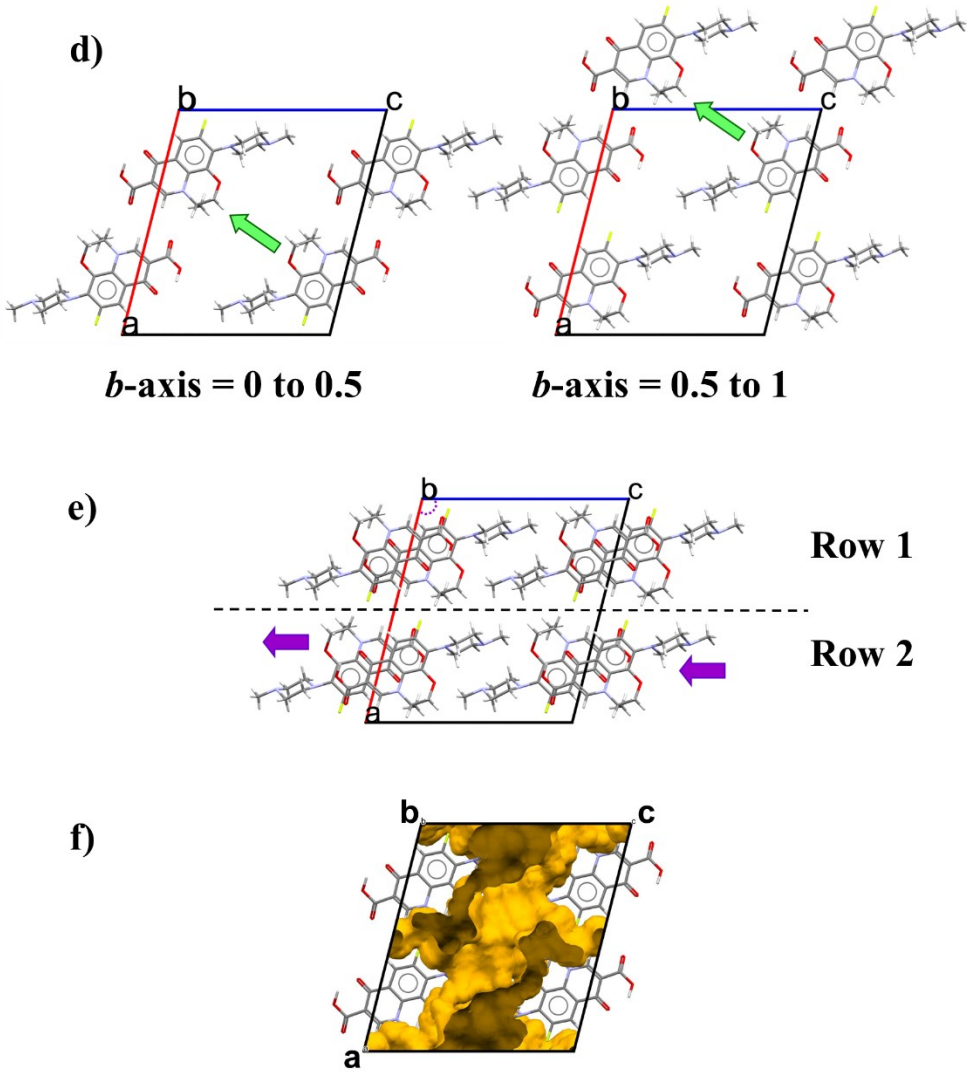

Figure S4 cont'd. d) Depiction of the direction of median principal compressibility (green arrow) in levofloxacin gamma; e) depiction of the impact of increasing β-angle in the unit cell of levofloxacin gamma; f) depiction of the voids in levofloxacin gamma at ambient pressure (LICWOM) (Mercury void analysis using 0.6 Å probe radius and a grid spacing of 0.2 Å).

Table S13. Table displaying the total lattice energies (E_{tot}) of ofloxacin as a function of pressure, along with the lattice energy components: Coulombic energy (E_{Coul}), polarisation energy (E_{pol}), dispersion energy (E_{disp}) and repulsion energy (E_{rep}). All energies are represented in kJ mol^{-1}. E_{tot} is corrected by considering the changes to the internal molecular energy. Pixel provides the values based on the intermolecular interactions and does not consider any change to the conformation of the molecule and the energy change that may arise from this change. The initial Gaussian calculation provides this, and the relative energies (from the ambient form) can be calculated and summed with the E_{tot} from Pixel.

Pressure (GPa)	**E_{Coul}**	**E_{pol}**	**E_{disp}**	**E_{rep}**	**E_{tot}**	**E_{tot} corrected**
CUYCEF	-70.9	-30.8	-157.4	101	-156	-156
0	-64.5	-38.1	-162.8	109.1	-149	-172.8
0.28	-72.8	-45.7	-181	138.6	-153.3	-168.0
0.76	-91	-53.7	-208.3	193	-152	-186.9
1.24	-102.4	-65.5	-228.2	238.4	-145.9	-180.3
1.81	-123.8	-69.6	-253.3	298.9	-143.7	-168.7
2.16	-130.5	-74.1	-261.8	320.8	-141.1	-167.8
2.47	-140.4	-85.7	-270.3	344.6	-140.1	-165.7
3	-161.5	-96.1	-290.7	408.5	-129.4	-154.4
3.62	-175.1	-109.2	-304.8	454.9	-121.1	-144.2
4.47	-195.8	-119.5	-323.5	524.2	-104.4	-124.2
5.2	-214.9	-115.4	-340.1	581.3	-93.2	-107.6

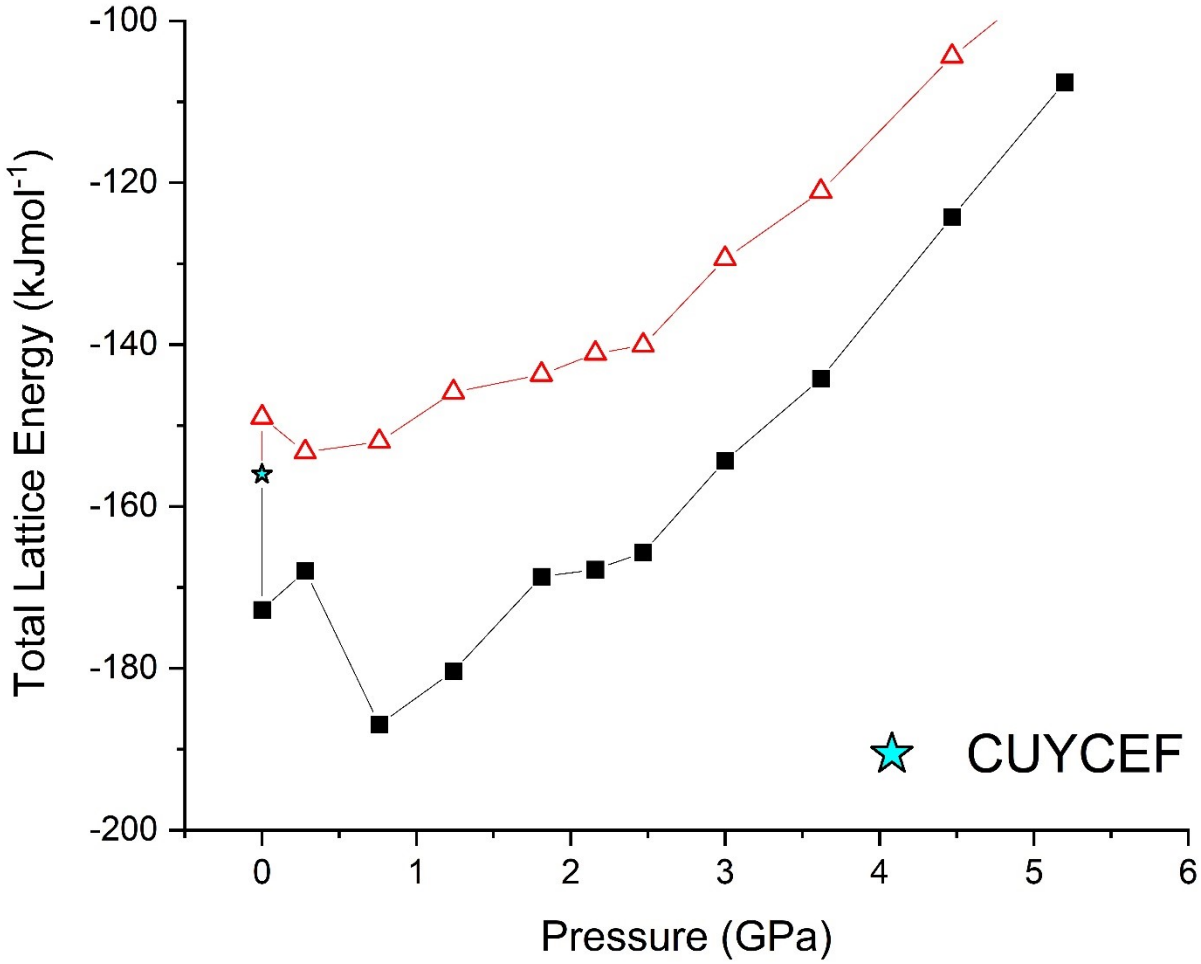

Figure S5. Total lattice energies of ofloxacin as calculated by PIXEL (red triangles) and total lattice energies of ofloxacin adjusted for the molecular energy due to conformational changes (black squares) relative to the ambient pressure configuration (CUYCEF).

S4. High-pressure X-ray Powder diffraction

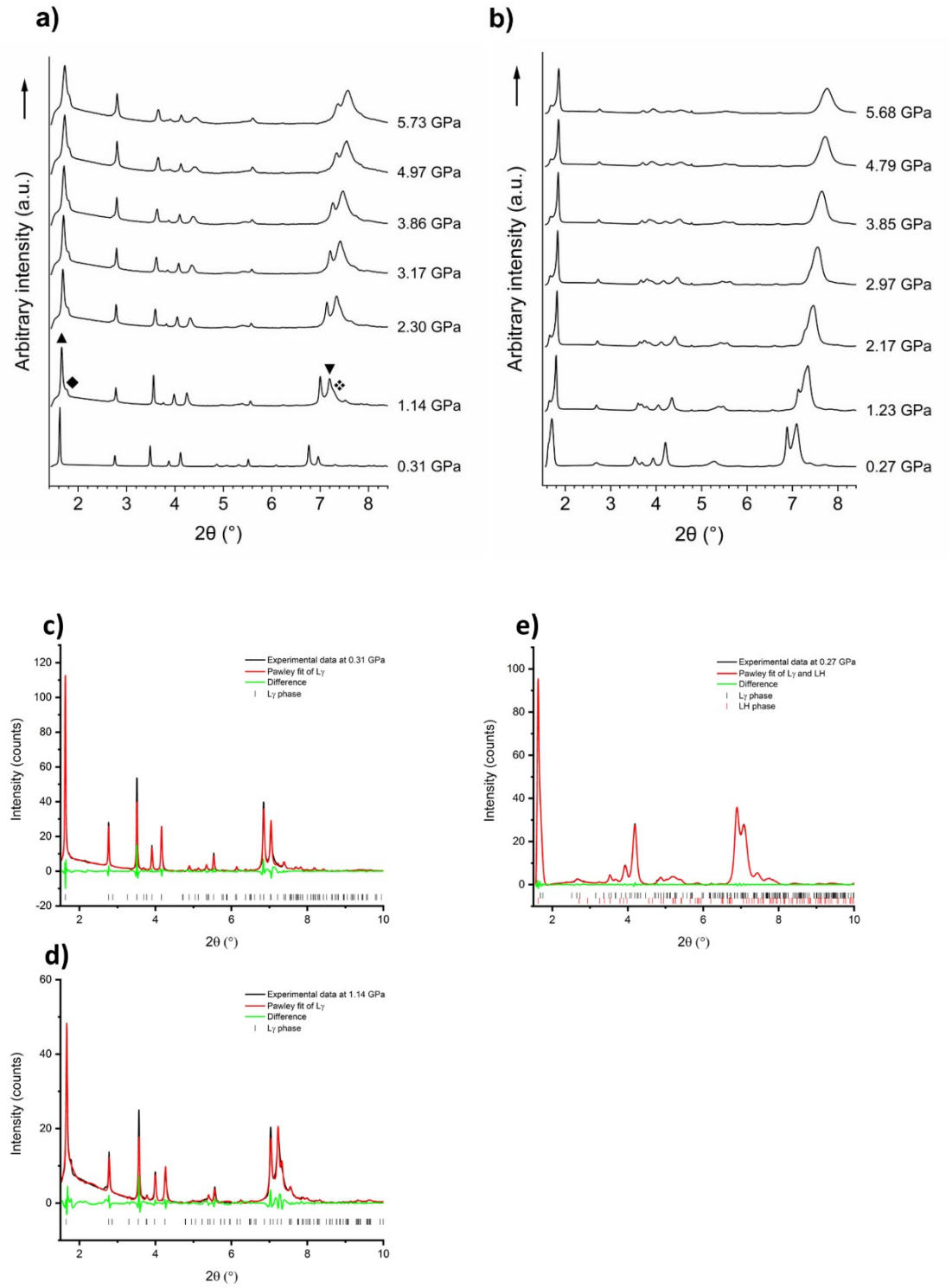

*Figure S6. Powder patterns during compression of γ-levofloxacin in (a) methanol–ethanol mixture and (b) petroleum ether. In (a), symbols indicate: ▲ (001), ◆ shoulder to (001) (corresponding to levofloxacin hemihydrate's (200) reflection), ▼ (021), ❖ shoulder to (021) (corresponding to levofloxacin hemihydrate's (021) reflection). In (b), the sample in petroleum ether appears to have transformed and is predominantly levofloxacin hemihydrate. The 2theta positions of the most intense peak below 2° and its shoulder do not match ▲ and ◆. Peaks between 3.5-4° and around 7° indicate that there is a substantial proportion of levofloxacin hemihydrate present. We have included the patterns for completeness to show the study was conducted but unsuccessful. c-d) Pawley fits to the data for γ-levofloxacin before and after transition indicating the misfits around the (001) reflection e) Pawley fit of the γ-levofloxacin in petroleum ether indicating the mixed phase with **LH.***

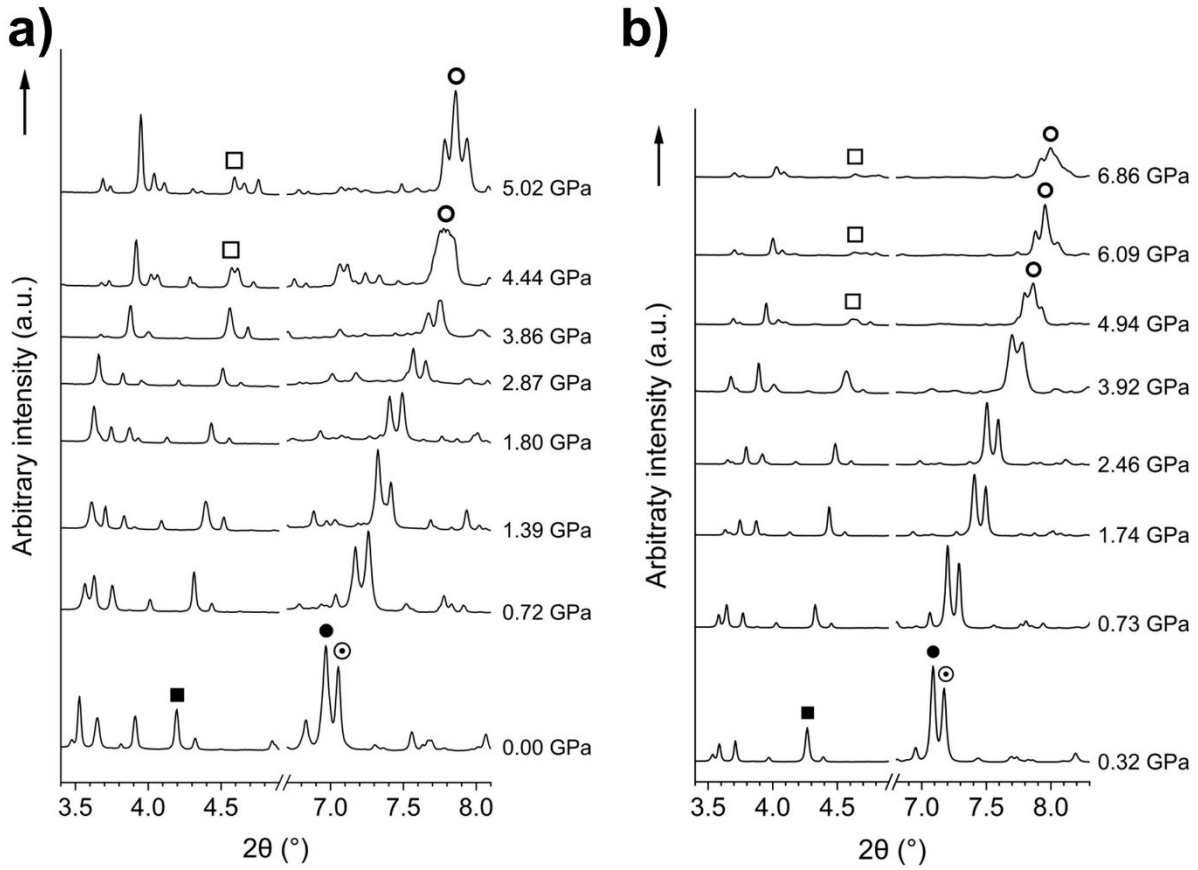

Figure S7. Powder patterns during compression of levofloxacin hemihydrate in (a) methanol–ethanol mixture and (b) petroleum ether. Symbols indicate: ■ ($31\bar{1}$), □ new peak neighbouring ($31\bar{1}$), ● (021), ⊙ ($22\bar{1}$), ○ new peak nestled between (021) and ($22\bar{1}$).

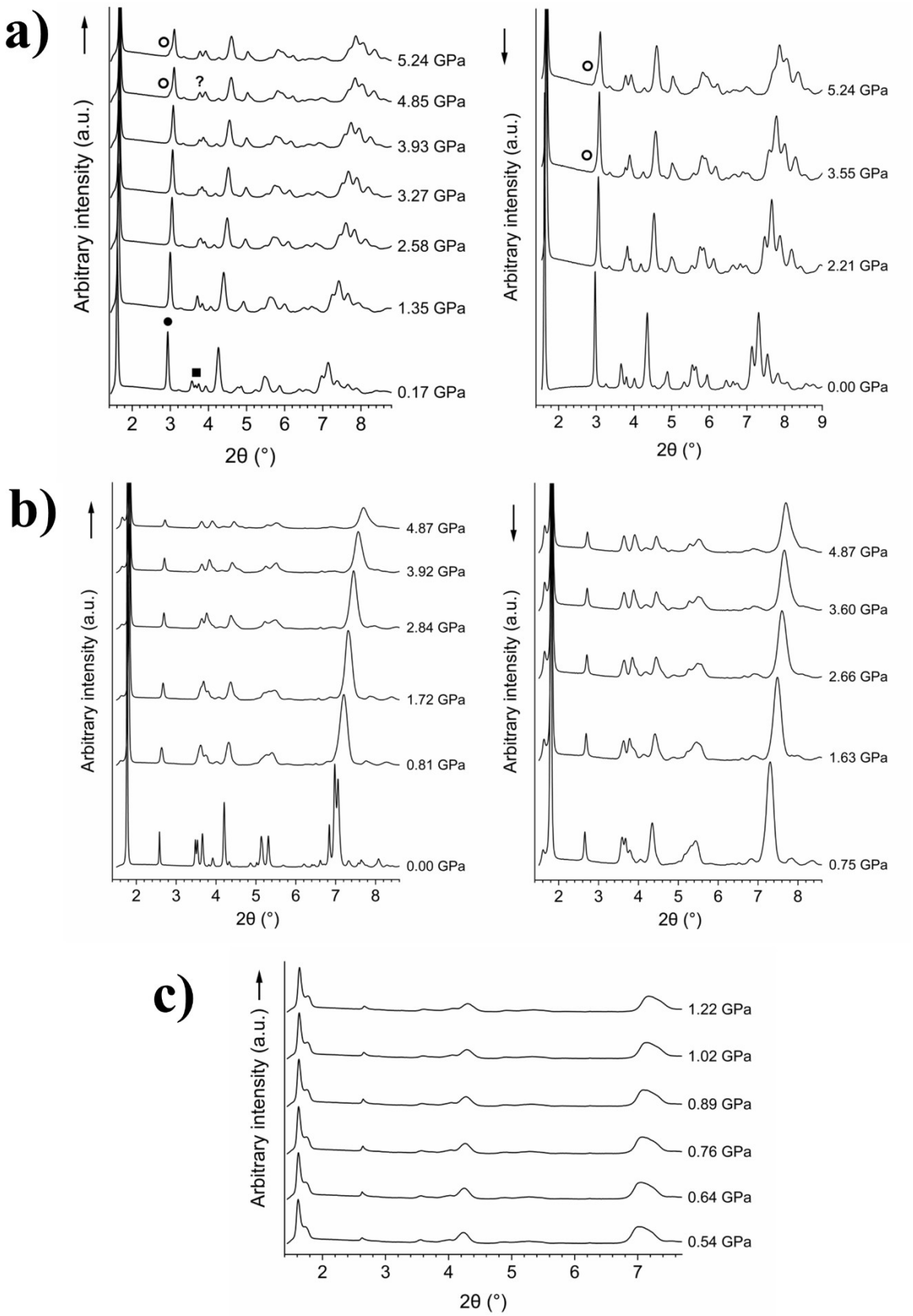

*Figure S8. Powder patterns during compression and decompression of (a) ofloxacin, (b) levofloxacin hemihydrate and (c) γ-levofloxacin without a pressure-transmitting medium. In (a), symbols indicate: ● (20$\bar{2}$), O new shoulder on (20$\bar{2}$), ■ (202), **?** no clear distinction of a new shoulder on (202).*

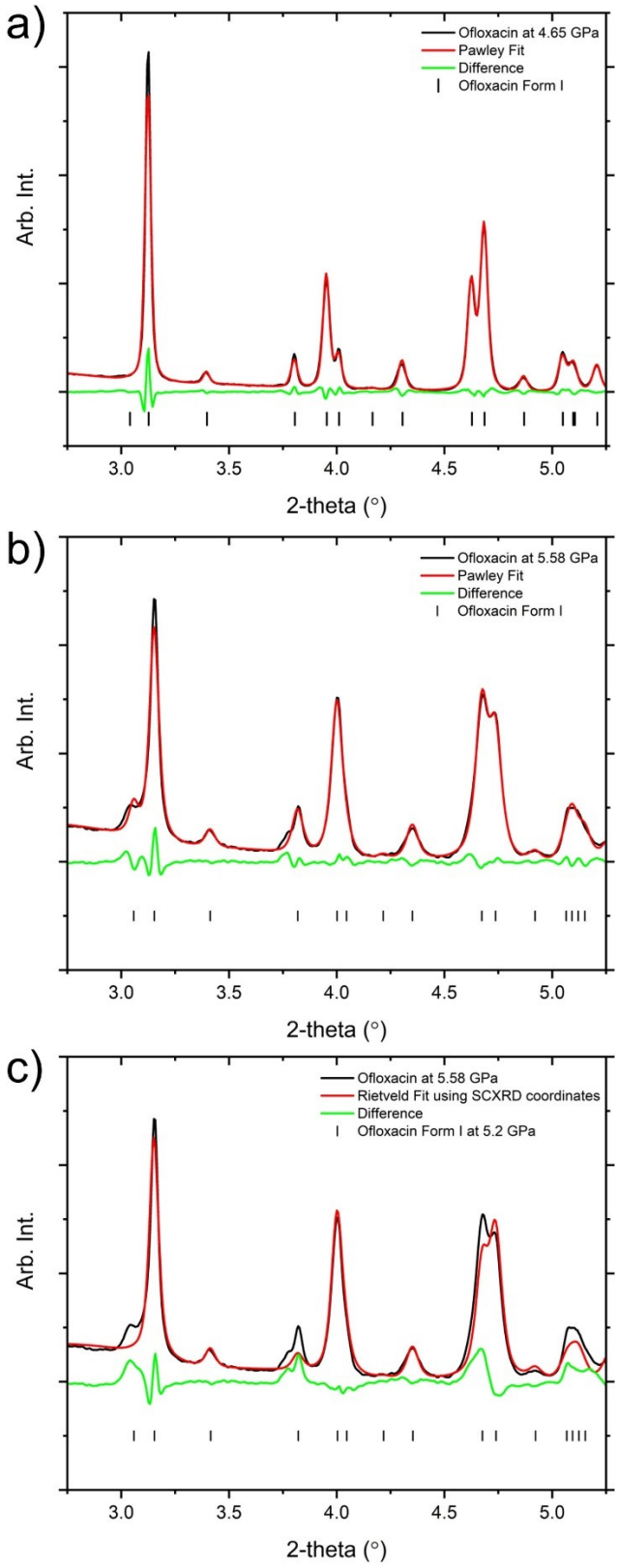

Figure S9. Fits to the ofloxacin data (a) below the transition and (b,c) above the transition in methanol–ethanol mixture. Both the Pawley and Rietveld fit are present for powder patterns above the transition to demonstrate that there is a new phase appearing with shoulder on the (20$\bar{2}$) and (2 0 2) reflections (3.06 and 3.77°). The coordinates of the structure determination at 5.2 GPa are used refining the Unit cell and scale factor and preferred orientation only. The Pawley fit uses the intensities of the pattern hence fits the peak at 3.06° but this intensity is not related to a change in the atomic positions.

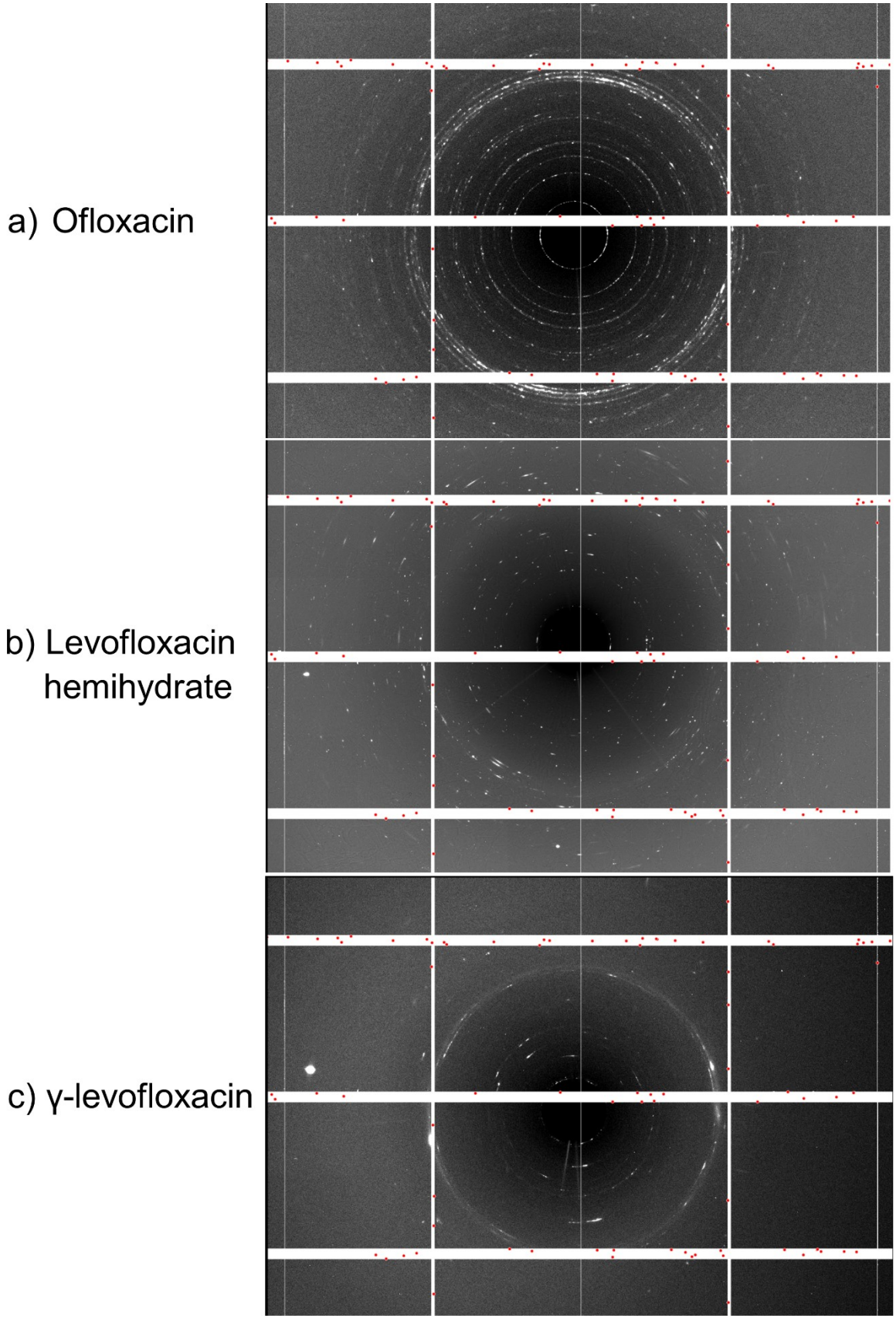

Figure S10. Raw images of the diffraction for (a) ofloxacin, (b) levofloxacin hemihydrate and (c) γ-levofloxacin in methanol–ethanol, indicating the poor powder averaging for the sample.